Isotherm Nonlinearity and Nonequilibrium Sorption Effects on Transport of Fenuron and Monuron in Soil Columns

FRANK C. SPURLOCK*

Department of Land, Air and Water Resources,
Hydrologic Sciences, University of California at Davis,
Davis, California 95616

KANGLE HUANG AND
MARTINUS TH. VAN GENUCHTEN

U.S. Salinity Laboratory, 4500 Glenwood Drive,
Riverside. California 92501

The influence of nonlinear sorption and prior sorbate/sorbent exposure time on transport of fenuron and monuron in laboratory soil columns was studied. Observed monuron breakthrough curves (BTCs) were well described using a two-region transport model with a single mass-transfer rate coefficient, independent of prior sorbate/sorbent exposure history. However, levels of soil-resident postelution monuron increased considerably with increasing exposure time, indicating increased sorption nonequilibrium with aging. Significant sorption nonequilibrium was observed for fenuron in spite of relatively high water solubility, low sorption, and relatively short sorbate/sorbent exposure time (ca. I-2 weeks). Sorption of fenuron was measured at solution concentrations up to the aqueous solubility limit. Batch data were reasonably well described by two distinct Freundlich isotherms depending *on* the concentration range. Accordingly, fenuron retardation factors varied significantly with concentration, displaying a minimum at intermediate concentration values. A comparison of linear and nonlineartransport modeling approaches suggests that failure to consider isotherm nonlinearity may be a source of considerable error when estimating nonequilibrium transport parameters from experimental BTCs.

Introduction

Experimental investigations of sorption and transport are important for understanding the fate and redistribution of chemicals in the subsurface environment. Although commonly assumed otherwise, sorption of organic compounds in soil is often nonlinear, i.e., the relative distribution of a chemical between the solution and sorbed phases varies as a function of the concentration being considered. Relatively few studies have examined the sorption of chemicals on soil at concentrations approaching the solubility limit. Such information may be needed to assess chemical transport in the vicinity of point sources.

Karickhoff et al. [1] reported sharp increases in sediment sorption of several aromatic and chlorinated hydrocarbons for equilibrium solution concentrations exceeding 60-70% of the sorbate solubility. Similarly, Walters and Guiseppi-Elie [2] found that sorption of 2,3,7,8-tetrachlorodibenzo-p-dioxin on soil from an aqueous methanol solution was linear up to approximately 50% of the solubility ($\sim 10^{-2}$ mg L^{-1}), but increased sharply at higher concentrations. Equilibrium sorption at the higher concentrations was described by the Freundlich isotherm

$$S = K_f C^N \tag{1}$$

with N ranging up to 1.5. In eq 1, S is the sorbed concentration (μg g^{-1}), C is the equilibrium solution concentration (μg mL^{-1}), K_f is the Freundlich constant (mL^N μg^{1-N} g^{-1}), and N is the Freundlich exponent (dimensionless). Because solute solution-phase activity coefficients for nonionic compounds of low solubility are essentially constant [3], these observations suggest a change in sorption mechanism at the higher concentrations. In contrast to the studies cited above, other researchers have reported sorption described by a single isotherm relationship up to near the solubility limits [4, 5].

One consequence of nonlinear sorption (N $\neq$ 1) is that the mobility of a compound becomes dependent on the concentration. The relative mobility of a solute during equilibrium transport may be described with the help of the retardation factor $R = 1 + (\varrho/\theta)(\partial S/\partial C)$, where ϱ is the soil bulk density (g cm^{-3}) and θ is the volumetric water content (cm^3 cm^{-3}). For miscible displacement of a column-resident solution ($C = C_i$) of a linearly sorbing solute by an influent solution of concentration C_0 ($C_i > C_0$), the retardation factor is equivalent to the area under the dimensionless experimental breakthrough curve (BTC)

$$R = \int_0^\infty C^* \, dPV \qquad C^* = \frac{(C - C_0)}{(C_i - C_0)} \tag{2}$$

where PV refers to pore volumes. Equation 2 can be derived using mass balance arguments similar to those used by Nkedi-Kizza et al. [6].

For the nonlinear case, $R = 1 + (\varrho K_f N / \theta) C^{N-1}$, which shows that the retardation factor is then concentration dependent. However, an effective retardation factor can still be approximated over a finite concentration range in any particular column experiment using the average slope of the isotherm, $\Delta S / \Delta C$ [7, 8]:

$$R = 1 + \frac{\Delta S \varrho}{\Delta C \theta}$$

$$\Delta S = S_i - S_0 \qquad (3)$$

$$\Delta C = C_i = C_0$$

This effective retardation factor for nonlinear sorption is also equal to the value of R calculated by eq 2.

The concentration dependence of R influences the shape of solute concentration curves versus distance (9) and time (10) because of variations in the effective solute velocity, v/R, with concentration, where v is the average porewater velocity (cm h^{-1}). When a relatively short solute pulse migrates through a soil column and N < 1, the solute front sharpens while the distribution behind the pulse displays more spreading relative to the linear case. This is manifested by increased tailing of elution BTCs at the higher pore volumes. Conversely, N > 1 results in less tailing. This influence on BTC shape can be important when attempting to estimate transport parameters from BTC shape.

The extent to which transport behavior in laboratory columns is descriptive of transport under field conditions is not clear, in part due to recent observations of the influence of sorbate/sorbent exposure time on the approach to desorptive equilibrium. A number of studies have observed that residues become more recalcitrant and slower to desorb with increasing exposure time to the sorbent (11-13). A recent column elution study by Pignatello et al. (14) found that freshly added herbicide was significantly more mobile than field-aged residue in the same soil. Because of these aging effects, the use of short-term batch experiments for describing sorption and transport in the field has been called into question (14-16). More studies examining the potential significance of aging behavior are needed since much of our current knowledge of sorption is based on short-term batch and column experiments. In this study, the effects of isotherm nonlinearity and prior sorbate/sorbent exposure time on the transport of two polar nonionic substituted phenylureas is examined.

Experimental Studies

Sorbents and Sorbates. The two soil samples (1 and 2) used in this study were collected from the A horizon (O-15 cm) of a Sycamore soil (fine-silty, mixed, nonacid, thermic inceptisol, Aeric Haplaquepts) field site in Yolo county, California. Textural characteristics and organic carbon are provided in Table 1. Details on sorbent preparation were reported previously (17).

Two moderately polar substituted phenylurea herbicides were used as chemical probes in this study: fenuron (1,1-dimethyl-3-phenylurea) and monuron (1,1- dimethyl-3-(p-chlorophenyl)urea). Solubilities and $\log_{10} K_{OW}$ are 3.9 g L^{-1}, 1.0, and 0.275 g L^{-1}, 2.12, for fenuron and monuron, respectively (18). Analytical determinations were conducted using reverse-phase HPLC (C-18 column, 58 and 42% aqueous methanol mobile phase for fenuron and monuron. respectively) in conjunction with UV detection (240 nm), while an aqueous dispersant/ethyl acetate partitioning method (17) was used for herbicide soil extraction.

Batch Sorption Studies. The 80-h batch isotherm studies are described in detail elsewhere (17, 18). In the case of fenuron sorption by soil 1 at the solubility limit, effluent from a generator column packed with 15 g of recrystallized fenuron was passed through a glass column containing ca. 50 g of soil 1 at a rate of approximately 0.2 mL min^{-1}. No detectable changes in column effluent concentration were observed after 40 pore volumes, and column equilibration was terminated after a total of 80 pore volumes (-5 days). The column was subsequently sectioned, the soil was extruded, and subsamples were taken for herbicide extraction and water content determination. The fenuron sorbed-phase concentration at the solubility limit was calculated by correcting total soil fenuron concentration for soluble fenuron using the measured column soil-water content and the terminal column eluant concentration.

Soil **Column Studies.** The soil column experiments were conducted using a 4.8 cm i.d. x 15 cm long preparative glass chromatography column (Kontes 420830-1530) equipped with adjustable end plates (Kontes 420836-0040), which permitted the use of variable soil column lengths. The columns were modified **by** replacing the manufacterer's plastic end plate frits with flat circular glass frits. PTFE/propylene O-rings were used to seal the end plates against the interior of the glass column. Dead volume between the end plates and the columnwall was minimized by tightly wrapping the circumference of the end plates with several layers of PTFE thread sealing tape. Fluid flow in the columns was vertically upward, and initial saturation of all columns was achieved using helium-purged solutions to reduce entrapped gas. Water contents were checked gravimetrically after initial equilibration periods and prior to termination of an experiment. The different influent solutions contained 0.4 g L^{-1} NaN_3 and 5 mM supporting electrolyte ($CaSO_4$ or $CaCl_2$) and were injected under constant flow conditions using an infusion/withdrawal pump. Previous experience has demonstrated the efficacy of NaN_3 for inhibiting microbial degradation of the two herbicides in soil suspensions over extended time periods (18). Effluent fractions were collected using an automated fraction collector.

Table 2 gives an overview of the different column transport experiments. In conjunction with the monuron and fenuron experiments, we also carried out displacements using chloride as an independent tracer as well as one chloride transport experiment with glass beads to test the overall performance of our displacement system. One monuron pulse input (experiment 1) and three monuron elution BTCs (experiments 2-4) were determined using soil 2. The elution BTCs were performed on samples that had been exposed to monuron for various periods of time (8, 80, and 240 days). For the the 8-day exposure period prior to initiating elution, a solution containing 103 μg mL^{-1} monuron was passed through the column for equilibration purposes. The 80- and 240-day monuron-contaminated soils were prepared by equilibrating 100 g of soil 2 with 150 mL of 5 mM $CaSO_4$ solution containing 0.4 g L^{-1} NaN_3 and 42 mg of monuron. At the end of incubation, the soil and solution phases were separated by centrifugation, and the supernatant was removed after sampling. The measured supernatant concentrations provided values of C_0 (initial resident solution concentration) for subsequent column experiments. The soil was subsampled for water content, allowed to air dry, passed through a 500-μm screen, subsampled for extraction and analysis, and packed into the glass soil column. After column equilibration for a minimum of 5 days, involving the leaching of between 80 and 100 pore **volumes** of monuron solution of concentration C_0, elution was initiated. Total monuron recoveries at the

TABLE 1

Selected Properties of Soils 1 and 2

soil	use history	clay (<2 μm)	silt (2–50 μm)	fine sand (50–126 μm)	coarsesand (>126 μm)	% oc
1	row crop >20 years	19	32	16	32	0.65
2	uncultivated grassland >20 years	32	56	13	0	3.42

TABLE2

Column Experimental Conditions

| expt no.	solute/expt	L(cm)	ρ (g cm^{-3})	e (cm^3 cm^{-3})	v (cm h^{-1})	φ_m[a]	D[a] (cm^2 h^{-1})	C_i (μg mL^{-1})	C_0 (μg mL^{-1})
1	monuron/soil 2	3.65	1.21	0.546	1.56	0.828 (0.820, 0.837)	0.063 (0.051, 0.075)	0	67.2
2	8-d monuron/soil 2	2.95	1.29	0.521	1.60	0.787 (0.776, 0.798)	0.181 (0.154, 0.208)	103	0
3	80-d monuron/soil 2	2.80	1.24	0.542	1.55	0.794 (0.784, 0.805)	0.115 (0.096, 0.134)	113	0
4	240-d monuron/soil 2	2.35	1.26	0.524	1.58	0.834 (0.824, 0.843)	0.140 (0.123, 0.156)	108	0
5	fenuron/soil 1	4.25	1.40	0.480	8.90	0.829 (0.819, 0.840)	1.11 (0.94, 1.27)	2880	329
6	fenuron/soil 1	4.25	1.40	0.480	8.90	0.829 (0.819, 0.840)	1.11 (0.94, 1.27)	375	35.8
7	fenuron/soil 1	4.25	1.40	0.480	8.90	0.829 (0.819, 0.840)	1.11 (0.94, 1.27)	45.0	4.30
8	fenuron/soil 1	4.25	1.40	0.480	8.90	0.829 (0.819, 0.840)	1.11 (0.94, 1.27)	5.25	0.53
9	fenuron/soil 1	4.25	1.40	0.480	8.90	0.829 (0.819, 0.840)	1.11 (0.94, 1.27)	1010	100
10	fenuron/soil 1	4.25	1.40	0.480	8.90	0.829 (0.819, 0.840)	1.11 (0.94, 1.27)	108	0

#Estimates and ±95% CI from chloride tracer BTCs using equilibrium linear convection dispersion equation (CXTFIT, 19).
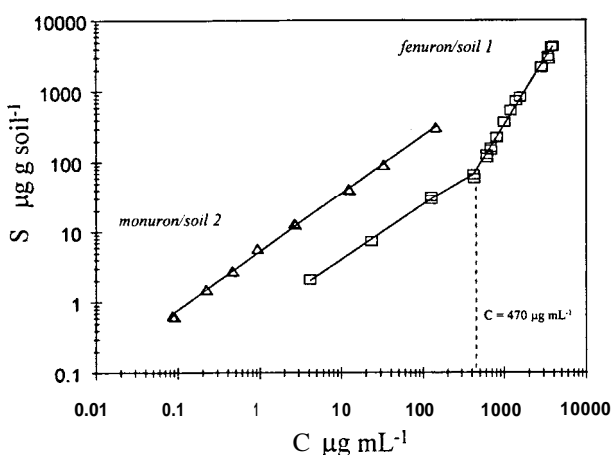
FIGURE 1. Batch equilibrium sorption data for fenuron on soil 1 up the solubility limit (3900 μg mL^{-1}) and monuron on soil 2 up to ca. 50% of solubility (142 μg mL^{-1}). Freundlich sorption parameters (eq 1) are $K_f = 0.664$ (mL^N μg^{1-N} g^{-1}) and N=0.781 forfenuron equilibrium concentrations less than 469 μg mL^{-1} (R^2 = 0.997, n = 6); K_f = 7.72 ×10^{-4} and N= 1.88 for fenuron equilibrium concentrations greater than 469 μg mL^{-1} (R^2 = 0.994, n = 23). Monuron/soil 2 parameters are K_f = 5.24. N = 0.824.

FIGURE 2. Fenuron K_{OC} (mL (g of OC)$^{-1}$) for fenuron/whole soil 1 (0.65% OC) sorption data (Figure 1) and fenuron sorption data for the <126-μm fraction of soil 1 (1.03% OC) reported by Spurlock (18).

end of incubation relative to the amount of monuron initially added ranged from 90 to 94%.

Six fenuron elution BTCs were conducted on the same packed column (experiments 5-10 in Table 2). Equilibration times for experiments 6-8 and 10 were approximately 60 h, with the water flow rate adjusted so that at least 60 pore volumes had passed through the column before the next elution step was initiated. The initial equilibration times for experiments 5 and 9 were 96 and 80 h, respectively. Chloride tracer BTCs determined prior to experiment 6 and after experiment 10 indicated no discernible changes in the column flow characteristics.

Transport Simulations. The BTCs were analyzed in terms of three one-dimensional transport models of increasing complexity. Two of these are based on the standard convection-dispersion equation describing transport of a sorbing solute in a homogeneous soil during steady-state water flow (e.g., van Genuchten et al., ref 20)
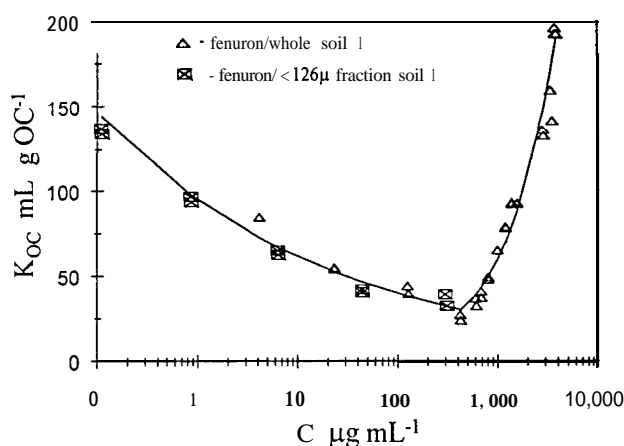
$$\frac{\partial C}{\partial t} + \frac{\varrho}{\theta}\frac{\partial S}{\partial t} = D\frac{\partial^2 C}{\partial x^2} - v\frac{\partial C}{\partial x} \qquad (4)$$

where x is distance, t is time, D is the dispersion coefficient (cm^2 h^{-1}), and v is the average porewater velocity (cm h^{-1}; equal to the fluid fluxdensity, q, divided by θ). This equation is valid irrespective of whether sorption is an equilibrium or a kinetic process.

The first model assumes nonlinear Freundlich equilibrium sorption (eq 1), in which case eq 4 reduces to

$$R\frac{\partial C}{\partial t} = D\frac{\partial^2 C}{\partial x^2} - v\frac{\partial C}{\partial x} \qquad (5)$$

where $R = 1 + (\varrho K_f N/\theta)C^{N-1}$ as before. Equation 5 was implemented here using sorption data (K_f and N) derived from independent batch equilibrium experiments, and estimates for D derived from chloride displacement experiments on the same soil columns at the same fluid flow velocities.
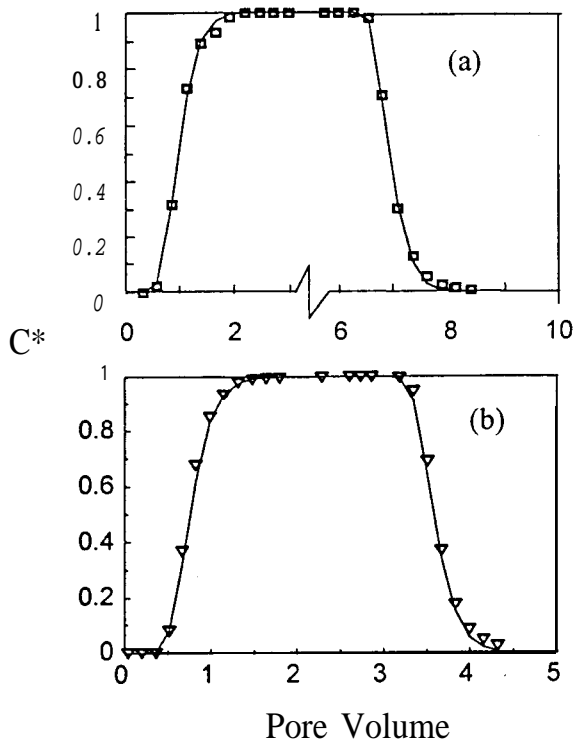
FIGURE 3. (a) Observed and fitted linear equilibrium BTCs for chloride transport in 100-μm glass beads. Column length L was 2.35 cm, V = 2.2 cm h^{-1}, θ = 0.394 $cm^3 cm^{-3}$, and the chloride retardation factor R and dispersion coefficient D as estimated by CXTFIT (19) were 1.00 and 0.20 $cm^2 h^{-1}$, respectively. (b) Observed and fitted linear equilibrium BTCs for chloride in column experiment 2 used to estimate φ_m (assumed equal to the chloride R, 0.787 for this BTC).

A second model assumes chemical nonequilibrium sorption for all sorption sites. The resulting one-site nonlinear nonequilibrium model is given by eq 4 with $\partial S/\partial t$ defined by the first-order rate expression

$$\frac{\partial S}{\partial t} = \alpha_1 (K_f C^N - S) \qquad (6)$$

in which $\alpha_1 (h^{-1})$ is a first-order kinetic rate constant. The only adjustable parameter is the rate coefficient α_1, which we estimated by trial and error from the experimental BTC data.

The third model considered here is the mobile-immobile (two-region) physical nonequilibrium transport model of van Genuchten and Wierenga (21) modified to account for nonlinear Freundlich type sorption. In this model, soil water is viewed as consisting of two regions: a mobile region associated with the larger conducting pores and a stagnant (non-moving) liquid region that does not contribute to water flow. The solid phase is similarly partitioned into a fraction f that equilibrates instantaneously with the mobile fluid, and another fraction (1 – f) that equilibrates with immobile liquid. Solute transfer between the mobile (subscript m) and immobile (superscript im) regions is modeled as an apparent first-order mass transfer process. The governing equations for the two-region model are as follows:

$$R_m \frac{\partial C_m}{\partial t} = D_m \frac{\partial^2 C_m}{\partial x^2} - v_m \frac{\partial C_m}{\partial x} - \frac{\alpha_2}{\theta_m}(C_m - C_{im}) \qquad (7)$$
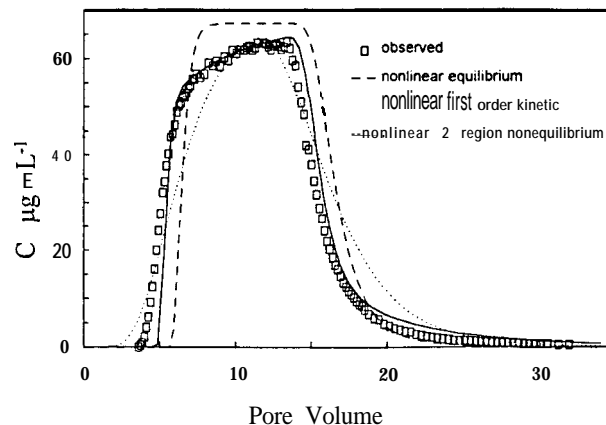

FIGURE 4. Observed and simulated short-term (-30 h) monuron pulse BTCs (experiment 1, Table 2). The one-site nonlinear nonequilibrium first-order rate constant α_1 = 0.6 h^{-1}; the two-region nonlinear simulation performed with α_2 = 0.08 h^{-1} and φ_m = 0.834 as estimated from the chloride tracer BTC.

$$R_{im} \frac{\partial C_{im}}{\partial t} = \frac{\alpha_2}{\theta_{im}}(C_m - C_{im}) \qquad (8)$$

where θ_m and θ_{im} are the water contents in the mobile and immobile zones such that $\theta = \theta_m + \theta_{im}$, $v_m = q/\theta_m$ is the average porewater velocity in the mobile zone, α_2 is a mass transfer coefficient (h^{-1}) describing the rate of transfer between mobile and immobile liquid phases, and R_m and R_{im} are retardation factors for the mobile and immobile zones, respectively.

$$R_m = 1 + f \frac{\varrho}{\theta_m} K_f N C_m^{N-1} \qquad (9)$$

$$R_{im} = 1 + (1 - f) \frac{\varrho}{\theta_{im}} K_f N C_{im}^{N-1} \qquad (10)$$

Following suggestions by Nkedi-Kizza et al. (22), among others, the two-region transport simulations shown in this paper were performed by assuming that $f = \varphi_m$, where $\varphi_m = \theta_m/\theta$ is the relative mobile water content as estimated from the observed chloride retardation factors. Consequently, the sole fitting parameter for the two-region simulations was the mass-transfer coefficient α_2.

The above models were solved subject to constant initial concentration conditions in the soil columns, third-type (flux) boundary conditions at the inlet of the soil columns, and a zero-concentration gradient at the column exit boundary

$$\left(-D\frac{\partial C}{\partial x} + vC\right)\Big|_{x=0} = vC_0$$

$$\frac{\partial c}{\partial x}\Big|_{x=L} = 0$$

$$C|_{t=0} = C_i$$

where L is the length of the soil column. These initial and boundary conditions also hold for the two-region model, provided C, v, and D are replaced by C_m, v_m ($= v/\varphi_m$), and D_m (= D/φ_m), respectively.

Numerical solutions of the above models were obtained with the finite element method using solution schemes as outlined by van Genuchten (23) but modified to include an

iterative solution process needed for treating the nonlinear retardation factors in the transport models.

Results and Discussion

Batch Sorption Results. Figure 1 illustrates the nonlinear sorption isotherms for fenuron on soil 1 and monuron on soil 2. Each isotherm spans 3 orders of magnitude in equilibrium solution concentration, with C ranging up to 50% and 100% of the aqueous solubility of monuron and fenuron, respectively. Fenuron sorption is described by two consecutive Freundlich isotherms depending on concentration. The fenuron octanol/water partition coefficient is independent of aqueous concentration up to at least 3000 g mL^{-1} (17), indicating that the fenuron aqueous-phase activity coefficient is relatively independent of concentration. Therefore, the sharp change in isotherm slope observed in the vicinity of C = 500 g mL^{-1} (S $\approx$ 80 μg (g of soil)$^{-1}$) indicates a change in fenuron sorbed-phase interactions. In the upper concentration region (N= 1.87), the isotherm increases smoothly up to the aqueous solubility limit where solid-phase fenuron is likely present in the soil. The unusual fenuron sorption process may be a result of induced crystallization in soil micropores or within the humic matrix at higher fenuron activities. Further studies will be required to evaluate this and other possible hypotheses.

Fenuron sorption data for the <126-μm fraction of sorbent 1 were previously reported (18). The combined sorption data (whole soil and <126-μm fraction) were used in Figure 2 to provide a plot of the fenuron single-point organic carbon normalized distribution coefficient (K_{OC}, mL (g of OC^{-1})) vs equilibrium aqueous concentration. Similar to the findings of Nkedi-Kizza et al. (24) for a related substituted phenylurea (diuron), sorption of fenuron was found to be relatively independent of particle size. The combined data illustrate that the fenuron K_{OC} (and hence, the fenuron single-point distribution coefficient, K_d, on sorbent 1) varies by a factor of more than 7 for solution-phase equilibrium concentrations ranging between 0.003% and 100% of aqueous solubility, displaying a minimum in the vicinity of C = 500 g mL^{-1}. The corresponding range for fenuron retardation factors on soil 1 is approximately 1.5-4.5 for tbe bulk density and water content of the column used for experiments 5-10.

Column Transport Results. Figure 3 shows BTCs for chloride movement in the glass bead column (Figure 3a) and column 2 (Figure 3b). The calculated curves were obtained using parameters fitted to the experimental data with the CXTFIT nonlinear parameter optimization program of Parker and van Genuchten (19). The effluent curve from the glass beads column could be described well with the convection-dispersion equation assuming no sorption (R = 1), while the description of the chloride data for soil column 2 improved only marginally when the two-region model with R = 1 was used. Note that the fraction of mobile water (φ_m, Table 2) in these columns was estimated to range from 0.79 to 0.83, indicating a relatively modest amount of immobile water.

The equilibrium nonlinear sorption transport simulations generally compared poorly with the observed data (e.g., see Figure 4 for an example): however, the agreement between simulated and observed BTCs improved markedly for all experiments when sorption nonequilibrium was introduced into the transport simulations. Although the two-region nonequilibrium model provided the best fits to
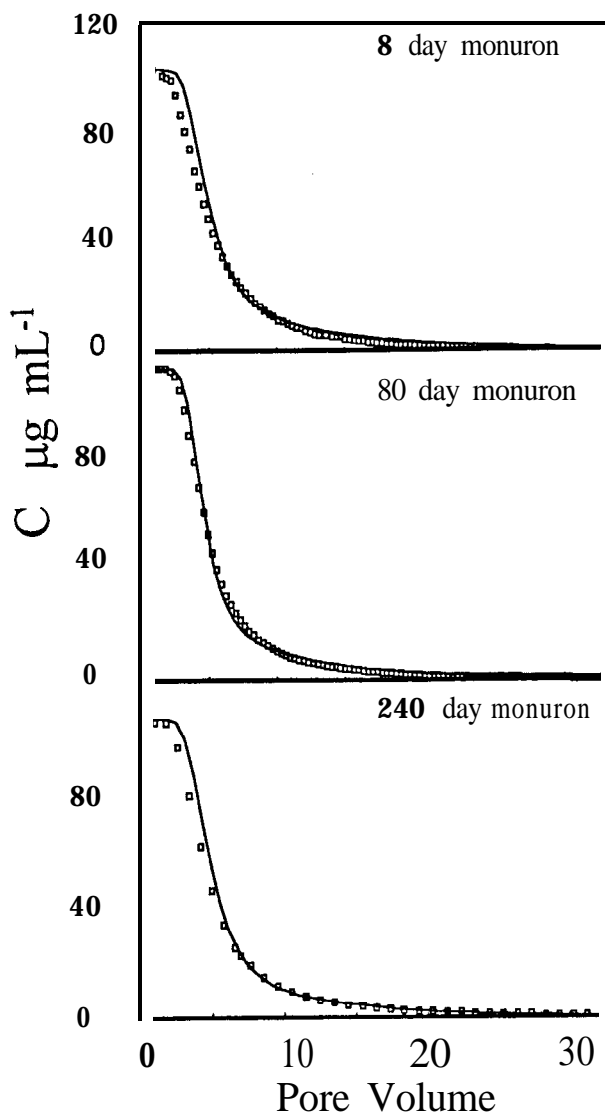

FIGURE 5. Monuron elution BTCs after different sorbent/sorbate exposure times (experiments 2-4, Table 2) prior to initiating elution and simulated BTCs using the nonlinear nonequilibrium two-region model. Simulated BTCs were calculated using α_2 optimized for short-term pulse (i.e., experiment 1, 0.06 h^{-1}) and φ_m = 0.787, 0.794, and 0.834 for experiments 2-4, respectively.

the data, goodness of fit should not be construed as validation of this model with regard to the underlying mechanism. As indicated by Nkedi-Kizza et al. (22), the relative contribution of grain-scale vs microscale diffusion processes (such as intraorganic matter diffusion) as well as kinetic processes cannot be accurately assessed using macroscopic observations.

Little effect on the elution BTC position or shape was observed with increased monuron/sorbent exposure time prior to initiating monuron leaching experiments 2-4 (Figure 5a-c) However, an increase in residual compound (i.e., the amount remaining in the column at the end of the experiments) was observed with increasing time of exposure of monuron to the sorbent prior to elution. Table 3 reports values of PV_T, S_T, C_T, S_{Eq}, and the ratio (S_T/S_{Eq}), where PV is the number of pore volumes and where the subscript T denotes measured values of the variables at the end of the different experiments when the relative concentration C* became less than about 0.01. The theoretical sorbed concentration S_{Eq} (= $K_F C_T^N$) in equilibrium with C_T was estimated from the 96-h batch equilibrium isotherm.

TABLE 3

Concentrations at End of Elution Experiments

experiment	elution time (h)	PV_T	$S_T{}^a$ (μg g^{-1})	C_T (μg mL^{-1})	$S_{Eq}{}^b$ (μg g^{-1})	S_T/S_{Eq}
no. 2/8-d monuron/soil 2	50	27	6.7	1.0	5.2	1.3
no. 3/80-d monuron/soil 2	59	33	14	0.69	3.3	3.9
no. 41240-d monuron/soil 2	49	32	23	0.81	4.4	5.2
no. 10/fenuron/soil 1	6.2	13	5.1	0.81	0.56	9.1

^{c}From extraction and analysis of soil at end of column experiments. b From 80-h uptake isotherms, Figure 1.
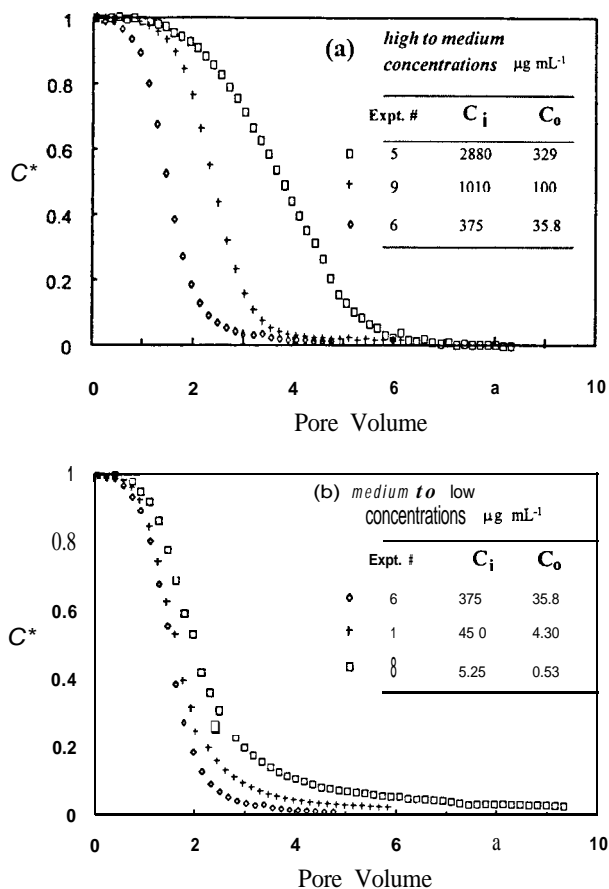

FIGURE 6. Fenuron decade step concentration elutions (experiments 5-9.Table2) conducted on the same packed column: (a) experiments 5, 6, and 9, high to medium concentration range elutions; (b) experiments 6,7, and 8. medium to low concentration range elutions.

Higher values of the ratio (S_T/S_{Eq}) at the end of the experiments indicate an increase in sorption nonequilibrium due to the influence of increasing prior sorbate/ sorbent exposure time. The residual monuron present in experiment 4 (240-day exposure time) was determined by extraction of different sections of the column and found to be evenly distributed throughout the column. The measured value of S_T in Table 3 corresponds to approximately 10% of the initial monuron sorbed-phase concentration (S_i) even though the terminal dimensionless eluant concentration C^*_T was <0.01. Assuming that the experiment had been continued and the monuron flux out of the column would not decrease further, elution of the residual monuron in experiment 4 would have taken an additional 80 pore volumes (-5 days). In reality, eluant concentration should steadily decrease further so that "complete" monuron elution from column 4 could have taken at least several hundred additional pore volumes. Corresponding elution times would have ranged upwards of several weeks at the imposed flow rate of 0.67 PV h^{-1}. Similar observations have

TABLE 4

Retardation Factors from BTCs and Estimated from Isotherms

expt no.	solute/sorbent	$R_{BTC}{}^a$	corrected $R_{BTC}{}^b$	R_{ISO} (95% CI)^c
2	8-d monuron/soil 2	5.96	6.22	6.68 (5.68, 7.89)
3	80-d monuron/soil 2	5.69	6.97	6.58 (5.60, 7.78)
4	240-d monuron/soil2	5.84	6.37	6.56 (5.58, 7.75)
5	fenuron/soil 1	3.74		3.73 (3.10, 4.52)
6	fenuron/soil 1	1.59		1.49 (1.35, 1.66)
7	fenuron/soil 1	1.84		1.78 (1.58, 2.00)
8	fenuron/soil 1	2.45		2.25 (1.90, 2.65)
9	fenuron/soil 1	2.29		2.02 (1.76, 2.33)
10	fenuron/soil 1	1.81	1.93	1.69 (1.56, 1.85)

^{a} Eq 3, upper limit of intergration = PV_T. ^{b} R_{BTC} corrected for measured residual compound at end of experiment. Corrected $R = R_{BTC} + (\varrho\, S_T)/(\theta\Delta C)$. ^{c} Eq 5, 95% CI based on 95% CI of S calculated from 80 h uptake isotherm.

been reported for elution of aged residues from soil columns by other researchers (14).

The fenuron decade step concentration elution experiments (i.e., $C_i \cong 10C_0$, experiments 5-9) shown in Figure 6 illustrate the marked dependence of the fenuron BTC position on absolute concentration due to isotherm non-linearity. As C_0 decreases, fenuron mobility first decreases and then increases, reflecting the shift in N from > 1 to < 1 around 500 μg mL^{-1} as observed in the batch experiments (Figure 2).

Table 4 reports retardation factors determined from integration of the observed BTCs (R_{BTC}, eq 2), corrected R_{BTC} values that account for the measured residual sorbed compound (S_T), and retardation factors calculated from the 96-h batch isotherm (R_{ISO}, eq 3). The agreement between the corrected R_{BTC} and R_{ISO} reflects the consistency of sorbed uptake concentrations predicted from the short-term equilibrium batch isotherms and those observed for the aged column soils.

Although fenuron displays relatively high aqueous solubility (ca. 3900 μg mL^{-1}, 18) and correspondingly low sorption, tailing of the fenuron BTCs was significant, particularly at the lower concentration ranges (Figure 6b). While best-fit first-order rate coefficients α_1 and α_2 were generally observed to change somewhat with concentration (being smaller at lower concentrations), the extent of sorption nonequilibrium cannot be quantitatively evaluated from the BTCs because $C_T{}^*$ is only a partial indicator of the degree of nonequilibrium of the sorbed phase. In addition to the apparent nonequilibrium effects as manifested by BTC tails, accurate evaluation of nonequilibrium transport parameters must consider the residual compound S_T left in the columns. Similar to the monuron experiments, extraction and analysis of the sorbent after the final fenuron elution experiment (experiment 10, $C_i = 0$) showed that even though effluent concentrations C* had decreased to
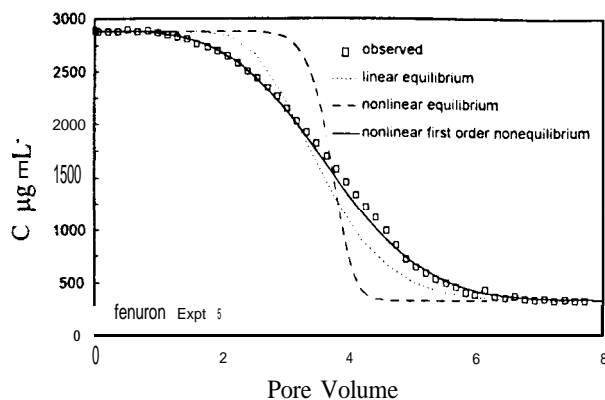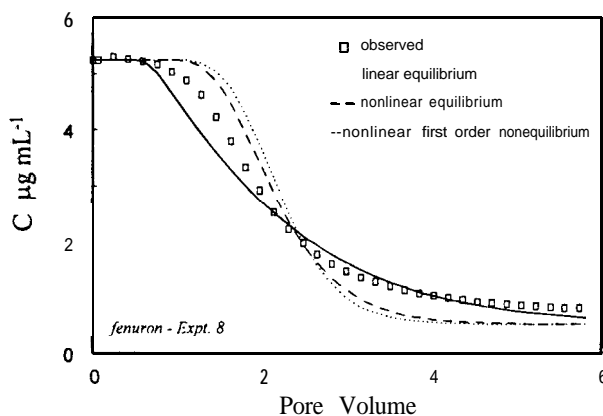
FIGURE 7. Column experiment 5 BTC data and linear equilibrium, nonlinear equilibrium, and nonlinear one-site first-order nonequilibrium simulations showing effect of isotherm nonlinearity (N = 1.88) on BTC tailing. The linear simulation was obtained using a retardation factor determined from nonlinear sorption data and eq 3; tbe nonlinear first-order nonequilibrium simulation used α_1 = 4.0 h^{-1}.

FIGURE 8. Column experiment 8 BTC data and linear equilibrium, nonlinear equilibrium, and nonlinear one-site first-order nonequilibrium simulations. The linear simulation was obtained using a retardation factor determined from nonlinear sorption data and eq 3; the nonlinear first-order nonequilibrium simulation used α_1 = 4.0 h^{-1}.

<0.01, significant amounts of residual fenuron remained in **the soil** columns. The postelution fenuron sorbed-phase concentration was 5 μg (g of soil)$^{-1}$, equivalent to approximately 20% of the resident compound prior to starting the final elution ($\approx$25 μg (g of soil)$^{-1}$, as predicted from the batch isotherm for C_i = 108 μg mL^{-1}).

The influence of isotherm nonlinearity on the BTC shape is shown in Figures 7 and 8. Comparisons of the linear and nonlinear simulations in the high concentration range (fenuron experiment 5, N = 1.87) illustrate the sharpening effect of nonlinear sorption on the elution BTC when N > 1. The sharpening effect is not directly evident from the experimental data, attributable in part to the concomitant influence of sorption nonequilibrium. In contrast, the linear and nonlinear simulations for experiment 8 in the lower concentration range show a broadening effect due to nonlinear sorption (N < l), although the effect is relatively small here because of the lesser nonlinearity (N = 0.78) at these concentrations. Still, the difference between the linear and nonlinear simulations may be significant from a transport modeling standpoint.

To illustrate the significance of nonlinearity to nonequilibrium parameter estimation, the linear and nonlinear equilibrium BTC simulations shown in Figure 8 were treated

as experimental data in order to obtain best-fit first-order rate coefficients (k_2, h^{-1}) in the two-site linear nonequilibrium transport model (19). Not surprisingly, the linear equilibrium simulation yielded a relatively high value for k_2 (165 h^{-1}) with large uncertainty (95% *CI,* ±30). In contrast, fitting of the linear two-site nonequilibrium model to the nonlinear equilibrium simulation yielded k_2 = 7.6 h^{-1}(±0.7, 95% CI), a value that is of comparable magnitude to those reported in the literature for organic compounds displaying similar sorption (25). This example illustrates that failure to account for even modest isotherm nonlinearity can have a significant effect on nonequilibrium transport parameter estimation.

The monuron data reported in this study are in general agreement with previous reports of increases in the slowly desorbing fraction with increasing sorbate/sorbent exposure time (11, 12). The fraction of slowly desorbing compound observed here was in the range of about l0-30%, considerably less than that observed by Pignatello et al. (12), who reported fractions of slowly desorbing atrazine and metalochlor in the range of 60 to more than 95% of S_i. Sorbate/sorbent differences notwithstanding, this apparent discrepancy may be a result of sorbent history. Pignatello et al. examined 7-month field-aged residues at much lower concentrations ($S_i \approx$ 0.2-0.6 μg (g of soil)$^{-1}$, where a relatively large portion of labile sorbate may have been removed by field transport or transformation processes prior to laboratory experimentation. Alternately, the fraction of slowly desorbing compound may also depend on concentration (26). Initial sorbed-phase concentrations for the monuron elution experiments ($\approx$200 μg (g of soil)$^{-1}$) were much greater than those in the study of Pignatello et al. (12) described above. In terms of absolute concentration, the slowly desorbing portion of sorbate ranged from 5 to 25 μg (g of soil)$^{-1}$ under the experimental conditions employed here. These levels could be significant from a toxicological or regulatory viewpoint.

Conclusions

Fenuron retardation factors were highly variable due to the influence of nonlinear sorption, displaying a minimum around S = 80 μg (g of soil)$^{-1}$, while fenuron single-point distribution coefficients (K_d) were observed to vary by a factor of -7. Retardation factors calculated from the observed BTCs were in approximate agreement with those calculated from batch experiments, indicating **the** suitability of short-term batch data for estimating sorptive uptake in these systems. While a nonlinear nonequilibrium transport model was able to simulate the observed BTCs down to effluent concentrations of less than 1%, the kinetic component of the elution/desorption process could not be fully characterized on the basis of short-term column experiments. Although BTCs were determined for relative concentrations ranging down to approximately 0.006-0.009, significant amounts of both fenuron and monuron remained sorbed in the columns after the elution experiments were terminated. The principal effect of exposure time on transport was an increase in the slowly desorbing portion of sorbate The compounds examined in this study consisted of polar nonionic organic compounds with relatively high solubilities. Since nonequilibrium sorption is generally considered to be most significant for strongly sorbing compounds, perhaps the most troublesome observation of this study is that significant nonequilibrium

was observed for the weakly sorbing, highly soluble fenuron, even for relatively short contact times (exposure times on the order of l-2 weeks). These results add to a mounting body of evidence that sorption nonequilibrium is a significant factor influencing the transport of organic compounds in soil. Further work is warranted to characterize the concentration dependence. temporal behavior, and mechanistic features of the slowly desorbing fraction.

Acknowledgments

literature Cited

(1) Karickhoff, S. W.; Brown, D. S.; Scott, T. A. *Water Res. 1979, 13, 241-248.*

(2) Walters, R. W.; Guiseppi-Elie, A. Environ. Sci. *Technol. 1988,22,* 819-825.

(3) Tsonopoulos, C.; Prausnitz, J. M. *Ind. Eng. Chem. Fundam. 1971, 10, 593-600.*

(4) Chiou, C. T.; Porter, P. E.; Schmedding, D. W. *Environ. Sci. Technol. 1983, 17, 227-231.*

(5) Rao, P. S. C.: Davidson. J. M. *Water Res. 1978. 13. 375-380.*

(6) Nkedi-Kizza,.P.: Rao, P. S.C.; Homsby,A. G. *Environ. Sci. Technol. 1987, 21,* 1107-1111.

(7) van der Zee, S. E. A. T. M. *Water Resow. Res. 1990, 10,* 2563-2578.

(8) Bosma, W. J. P.; van der Zee, S. E. A. T. M. *Transp. Porous Media 1993, 11,* 33-43.

(9) van Genuchten, M. Th.; Cleary, R. W. *In Soil Chemistry B, Physico-Chemical Models, Developments in Soil Science 5B;* Bolt, G. H., Ed.; Elsevier: Amsterdam. 1979; pp 349-386.

(10) Brusseau, M. L.; Rao. P. S. C. *Crit. Rev. Environ. Control 1989, 19,33-99.*

(11) McCall, P. J.;Agin, G. L. *Environ. Toxicol. Chem. 1985,4,37-44.*

(12) Pigantello J. J.; Huang, L. Q. J. *Environ. Qual* 1991, 20 222-228.

(13) Coates, J. T.: Elzerman. A. W. J. *Contam. Hvdrol.* **1986. 1. 191-**210.

(14) Pignatello, J. J.; Ferrandino, F. J.; Huang, L. Q. *Environ. Sci. Technol.* **1993,** 27, 1563-1571.

(15) Ball, W. P.; Roberts, P. V. *Environ. Sci. Technol.* **1991.25.** 1223-1237.

(16) Ball, W. P.; Roberts, P. V. *Environ. Sci. Technol.* **1991,25, 1237-1 2 4 9 .**

(17) Spurlock, F. C.; Biggar, J. W. *Environ. Sci. Tcchnol. 1994, 28, 996- 1002.*

(18) Spurlock, F. C. Ph.D. Dissertation, University of California at Davis, 1992.

(19) Parker, J. C.; van Genuchten, M. Th. *Determining transport parameters from laboratory and field tracer experiments;* Bulletin 84-3; Virginia Agricultural Experimental Station: Blacksburg, VA, 1984; 96 pp.

(20) van Genuchten, M. Th.; Davidson, J. M.; Wierenga, P. J. *Soil Sci. Soc. Am. Proc.* **1974,** *38, 29-35.*

(21) van Genuchten, M. Th.; Wierenga, P. J. *Soil Sci. Soc. Am. J.* **1976,** *40, 473-480.*

(22) Nkedi-Kizza, P.; Biggar, J. W.; Selim, H. M.; van Genuchten, M. Th.; Wierenga, P. J.; Davidson, J. M.; Nielsen, D. R. *Water Resour. Res.* **1984,20,** 1123-1130.

(23) van Genuchten, M. Th. *Adv. Water Resour.* **1982,** 5, 47-55.

(24) Nkedi-Kizza, P.; Rao, P. S. C.; Johnson, J. W. *J. Environ. Qual.* **1983,** *12.* 195-197.

(25) Brusseau, M. L.; Rao, P. S. C. *Environ. Sci. Technol.* **1991, 25, 1501-1506.**

(26) Pignatello, J. J. *Environ. Toxicol.* Chem. 1990, 9, 1117-1126.